A characterization of PMTs for the new IceCube mDOMs

Bachelorarbeit aus der Physik

Vorgelegt von
Paul Lehmann
14.01.2020

Physikalisches Institut
Erlangen Centre for Astroparticle Physics
Friedrich-Alexander-Universität Erlangen-Nürnberg

Betreuerin: Prof. Dr. Gisela Anton

Contents

1 Motivation

In the year 1930, Wolfgang Pauli proposed the idea of the particle we today know as the electron neutrino: a chargeless particle that allowed preservation of spin, impulse and energy during the beta decay.

Neutrinos are a family of particles from the group of fermions. They have a spin of $\frac{1}{2}$, but carry no electric charge, and the upper limit of their mass has been determined to be several orders of magnitude smaller than that of an electron. As they only interact via the weak force, their interaction cross section is very small. These properties make them one of the most promising messengers in high energy astrophysics, as their trajectories can be reconstructed directly to their sources. These are supposed to be the high energy accelerators the astrophysics community is interested in.

On the adverse, their small cross section also means that detecting neutrinos is quite challenging, as huge detector volumes are mandatory to overcome the problem of low flux combined with the low cross section. This requires a choice of detector material that is abundant and cheap, and offers means to reduce background inevitably found in such a large volume. A natural candidate that fulfills these criteria is ice, specifically the antarctic ice, which is being instrumented by the IceCube Neutrino Observatory.

The detection method chosen is to measure Cherenkov light emitted by secondary particles, which are created upon interaction of an astrophysical neutrino with the ice surrounding the detector. To make use of detected signals, the sensor response is of great importance. Additionally, the south pole exhibits climatic conditions that are somewhat divergent from laboratory conditions.

Therefore, this thesis aims at investigating the basic detector unit, the photomultiplier tubes that will be used for the mDOM which is the baseline sensor for the IceCube Upgrade.

2 Introductory Considerations

This chapter aims to introduce the general concepts relevant for this thesis.

2.1 The IceCube experiment and upgrade

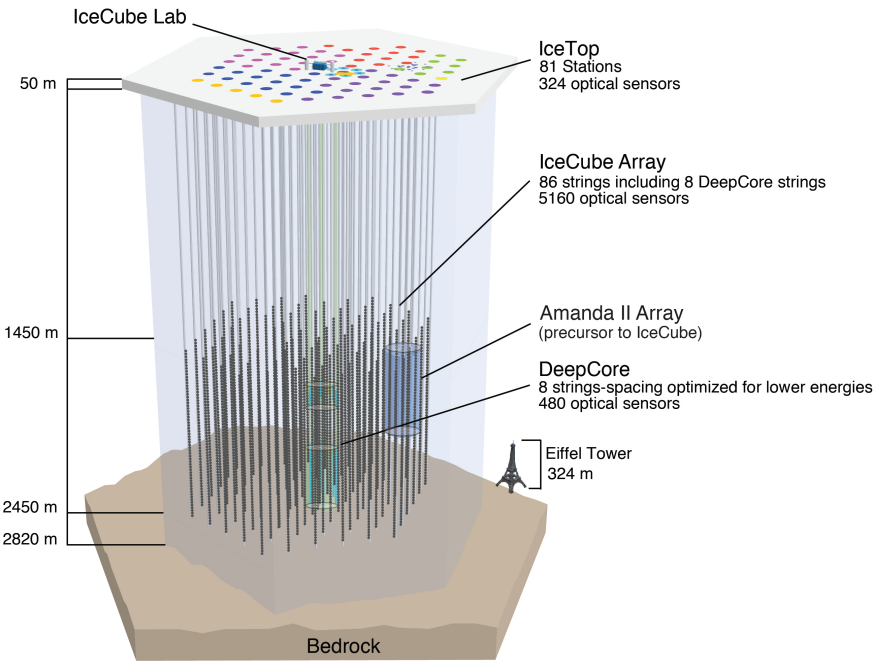

Figure 1: *Artist's impression of the IceCube Neutrino Observatory. Taken from [6]*

The IceCube experiment, which in its current form was completed in 2010, is an ice Cherenkov detector located at the South Pole. It currently consists of 86 strings positioned vertically in the polar ice in a hexagonal pattern, each of which reaches a depth of 2450 m under the surface (see Figure 1). Between the strings, the horizontal distance is 125 m. The ice at these depths is both clear and dark, therefore providing good conditions for low light-level measurements. The detector encompasses a volume of roughly a cubic kilometer of ice. [4] [7]

Each string holds 60 so called Digital Optical Modules (DOMs), the fundamental sensor units of IceCube, distributed on the string with a vertical distance of 17 m between DOMs. Each DOM holds a 10" photo multiplier

tube (PMT) - the Hamamatsu R7081-02 - oriented downwards as actual sensor, as well as electronics for data acquisition and operation of the PMT.

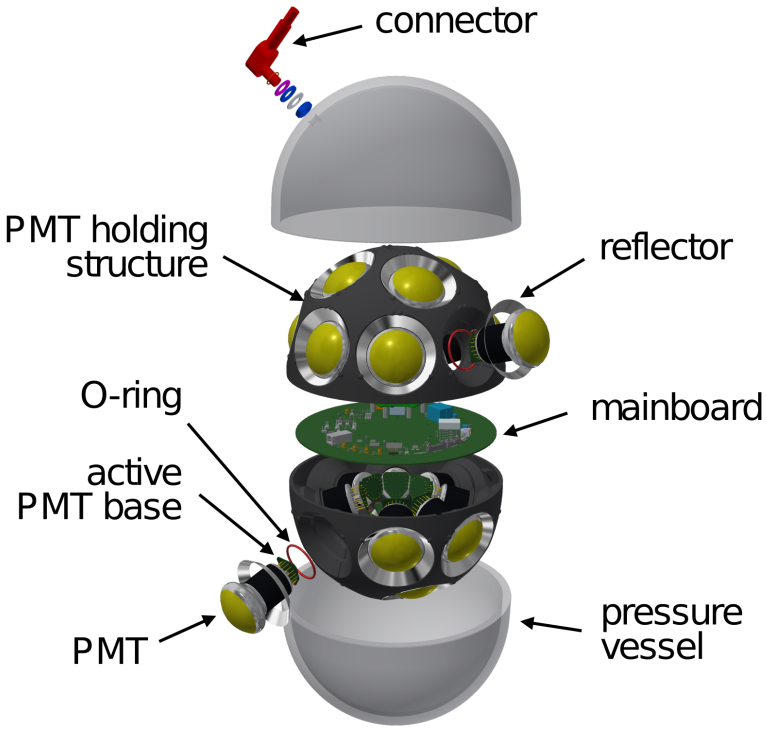

Figure 2: *Artists impression of an mDOM for the IceCube Upgrade. Adapted from [9]*

.

As neutrinos travel through the ice, they have a chance to interact with the ice and create a cascade of secondary particles - a particle shower. These showers continue interacting in the ice. Since their speed of travel is higher than the speed of light in ice, they emit light through the Cherenkov effect. This light is the primary signal IceCube is looking for. IceCube is sensitive to primary neutrino energies of 10 GeV to 10 PeV.

In addition, eight strings in the center of the detector are instrumented more densely comprising the DeepCore array. Their DOMs are deployed at a lower altitude and contain PMTs with higher quantum efficiency. These serve to considerably lower the energy threshold of detection, by a factor of up to ten compared to the regular modules. Detection is optimized in the range of 10 GeV to 100 GeV.

Furthermore, the IceCube experiment contains the IceTop array: An array of surface level tanks filled with ice and two DOMs respectively. These tanks'

purpose is to detect airborne particle showers, beginning at roughly 100 TeV up to EeV range.

The combination of IceCube, DeepCore and IceTop allows the experiment to cover the entire "knee" of the cosmic ray spectrum, and into a range that may even contain extra-galactic cosmic rays.[4]

To expand on the success that IceCube had so far, the IceCube upgrade is currently in development. This evolution will consist of seven new strings carrying the new Multi-PMT Digital Optical Modules (mDOM, see Figure 2) and Dual optical sensors in an Ellipsoid Glass for Gen2 (D-Egg), located in the bottom center of the existing IceCube array. These new modules will possess PMTs with higher efficiency, which, along with their dense clustering of 20 m horizontal and 3 m vertical distance, will increase the array's sensitivity in the range from 1 GeV to 10 GeV.[5]

An additional improvement of the IceCube array, the Gen2 upgrade, is also in the early planning phase. This project aims at dramatically increasing the detector volume of the IceCube array by around 8 km^3 through the addition of less densely spaced detector strings.[3]

2.2 Technical description of a PMT

Central element of the IceCube detectors are the PMTs used for signal detection. Their fundamental purpose is to detect light, down to signals consisting of single photons, and convert this light into an electrical signal fit for further processing.

Fundamentally, they are evacuated glass tubes with an entrance window coated with photocathode material responsible for photon-electron-conversion, behind which there is a dynode system responsible for signal amplification. (See Figure 3 for an exemplary schematic.) Photons hitting the photocathode have the potential to trigger a photo emission by imparting their entire energy onto a bound electron of the cathode material, allowing it to leave the material. In the Hamamatsu R12199-01HA, the cathode consists of a bi-alkali material, although silver-oxygen-cesium, antimony-cesium, tri-alkali-compounds, and even non-opaque semi-conductors are also materials that can be used.

While the released electrons may have a small velocity upon leaving the cathode, a positive potential is applied to accelerate and focus them towards the electron multiplier that makes up the second part of the PMT. This electron multiplier consists of a number of dynodes, each at a higher potential than the one before it. This causes an electron to be accelerated between dynodes. Upon impact on the dynode, this kinetic energy causes emission of secondary electrons, which in turn get accelerated to the next dynode, achieving the desired amplification of the initial electron(s). Dynode systems

will often have complex geometrical configurations to maximize gain.

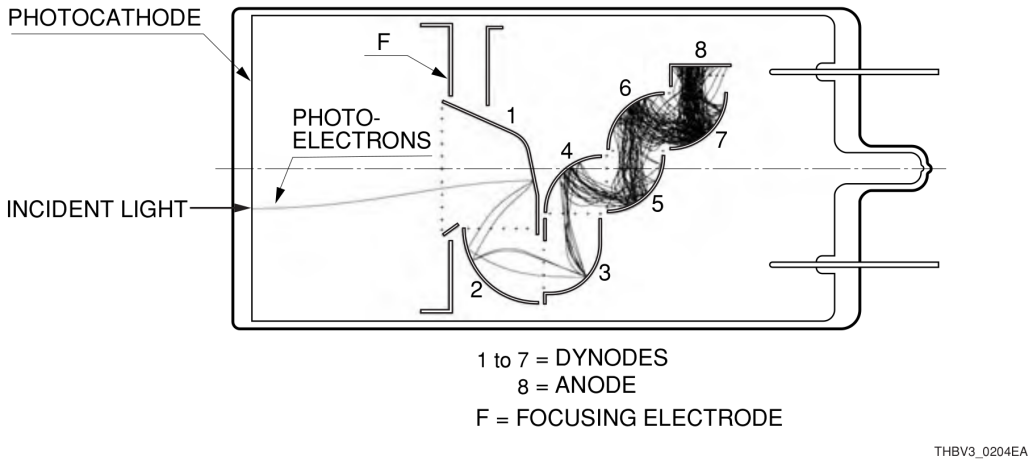

Figure 3: *Composition of a PMT. IceCube's Hamamatsu PMTs use the dynode setup shown. Adapted from [2]*

The distribution of dynode potential is determined by a voltage divider in the PMT's base. While this base is not part of the PMT itself, it is still essential for PMT operation, as the resistor strength in the divider, and through them the dynode potential, are directly responsible for the dynode's actual gain factor. As it is often desirable to operate under a constant, normalized gain, by convention the Nominal Voltage of a PMT is the amount of voltage that must be applied to its voltage divider to achieve a certain gain. [8]

The electrons leaving the last dynode are then collected by the anode, from which the signal then is collected.

2.3 PMT signal

There are generally two approaches to measure the final signal, both of which are used in the scope of this thesis:

- In *current mode*, the electron current can be measured directly as a current. Integrating over the range of time in which a signal is expected, the signals total charge can be determined, but little else.
- Alternatively, the current can be applied to a resistor - such as the entrance resistor of an oscilloscope - and the resulting voltage can be measured. This so called *pulse mode* allows insights into more detailed characteristics of the signal, such as transit time spread.

To understand the shape of a signal measured in pulse mode, it should be noted that neither the initial photo emission, nor absorption by the respectively next dynode are assured, but rather are statistical processes.

Emission of the initial photoelectron and collection into the dynode system are random binary processes that can collectively be described with a Poisson distribution:

$$P(n;\mu) = \frac{\mu^n \mathrm{e}^{-\mu}}{n!} \tag{1}$$

,

with μ being

$$\mu = mq \tag{2}$$

,

with the probability $P(n;\mu)$ that n photoelectrons are observed, the mean being μ observed electrons, m the mean number of photons hitting the photocathode, and q the quantum efficiency of the photocathode. [1]

The response of the dynode system to a single electron can be described by a Gaussian distribution

$$G_1(x) = \frac{1}{\sigma_1\sqrt{2\pi}} \exp\left(-\frac{(x-Q_1)^2}{2\sigma_1^2}\right) \tag{3}$$

,

where x is the variable charge, Q_1 is the average charge arriving at the output anode for a lone collected photoelectron, and σ_1 is the corresponding standard deviation of the single electron distribution. This description, however, requires a large (> 4) amount of electrons emitted from the first dynode - i.e. a high potential between the photocathode and the first dynode - and a collection efficiency of later dynodes close to 100 %. [1]

As the amplification of multiple electrons can be assumed to not interfere with each other, the response to a n photoelectron case can be described as the convolution of n single electron response functions[1] :

$$G_n(x) = \frac{1}{\sigma_1\sqrt{2\pi n}} \exp\left(-\frac{(x-nQ_1)^2}{2n\sigma_1^2}\right) \tag{4}$$

The third element of the PMT response is created by background processes. Both processes caused as a result of initial photons, and processes independent of any signal - such as thermal electron emission, leakage currents, or internal radioactivity - contribute to this background.

Background response can be split into two parts:

- Processes that cause a small charge to be detected despite absence of initial photoelectrons. These processes can be described by a Gaussian distribution around the 0 charge point. This additional Gaussian is called the pedestal. Its primary cause is electrical noise.

- Processes that can offset an already existing signal, such as additional thermal emission, or electrons missing the first dynode but impacting a later one. These processes can be described by a falling exponential function.

[1]

Thus, the background can be described as

$$B(x) = \frac{(1-w)}{\sigma_0\sqrt{2\pi}} \exp\left(-\frac{x^2}{2\sigma_0^2}\right) + w\theta(x)a\exp\left(-ax\right) \tag{5}$$

with σ_0 being the standard deviation of the pedestal background, w the probability that any given signal is modified by the exponential background process, and a the coefficient describing the decrease of the exponential background.

$$\theta(x) = \begin{cases} 0 & x < 0 \\ 1 & x \geq 0 \end{cases}$$

is the step function that sets the exponential background to zero for charges lower than 0.

A realistic response function will be a convolution of Equation 1, Equation 4, and Equation 5. [1] For an example of actual pulse shape data with fitted pedestal and single photon Gaussian, see Figure 4.

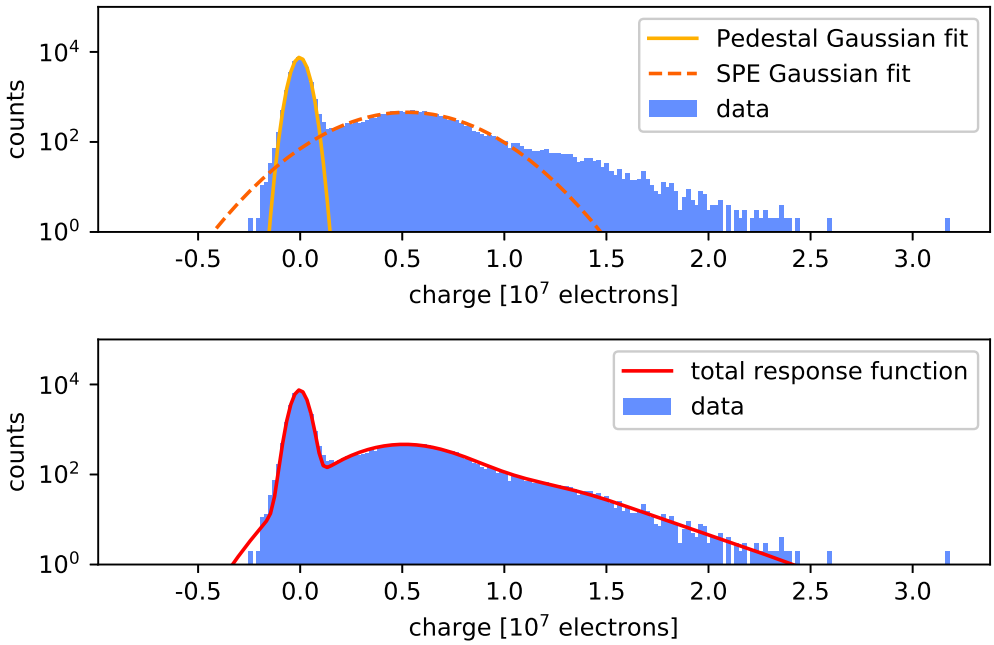

Figure 4: *Example of a signal measured in pulse mode at nominal voltage.*
Above: *A Gaussian (yellow) for the pedestal background and Gaussian (orange, dashed) for the single photoelectron event (also called SPE) have been fitted to the data.*
Below: *The entire response function (red) has been fitted. It is derived from the two Gaussians above by adding a number of additional Gaussian distributions for the respective n-photoelectron events.*

3 Temperature dependent gainslope of an HZC PMT

To investigate the influence of temperature on signal gain, a series of gainslopes under different temperatures is recorded. The detectors of IceCube can encounter temperatures as low as −20 °C, which makes understanding the impact of temperature on detector behavior a necessity.

Setup

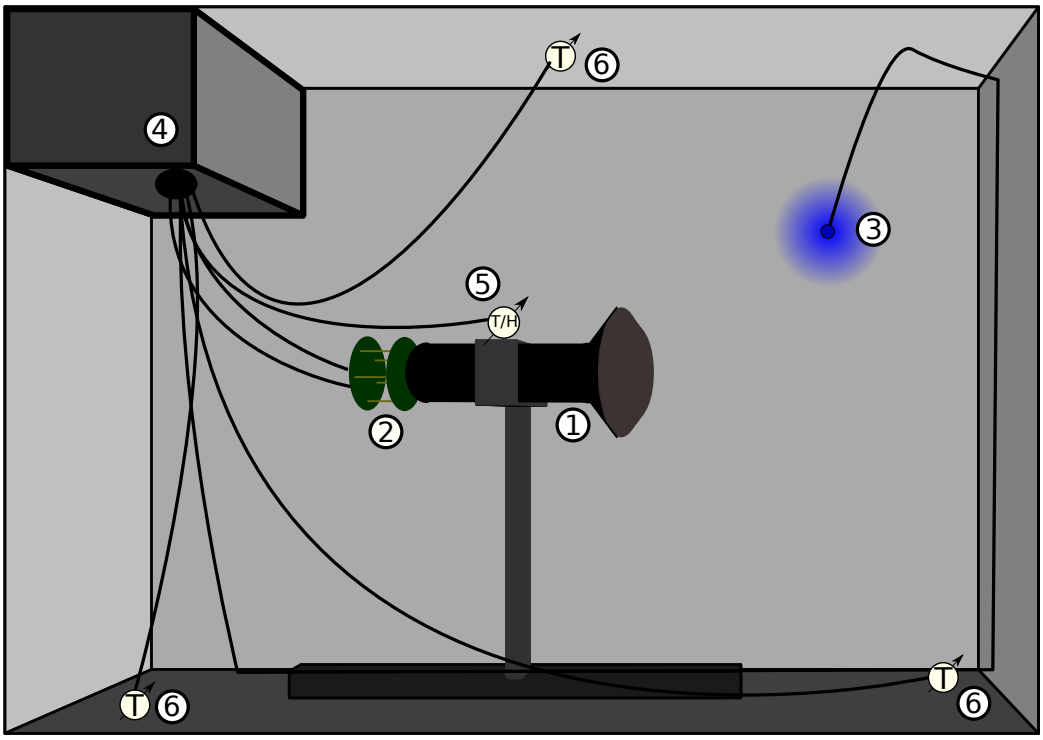

Figure 5: *Schematic of the interior of the dark box. The black foam has been omitted for readability purposes. 1: PMT, 2: base, 3: LED, 4: light trap, 5: temperature/humidity sensor, 6: temperature sensor*

For exact specifications and settings of equipment used, see section A.

The experimental part of the setup is located within a dark box lined with black foam of roughly 5 mm thickness (see: Figure 5. The foam serves to absorb stray light and therefore reduces background. The PMT and its base are mounted roughly centrally in the box, in a bracket mounted on an

optical rail system. It is supplied by a high-voltage source. Data-taking is accomplished by an oscilloscope connected via coaxial cable, which in turn is read out by a PC via LAN connection.

A generic, commercially available blue LED is attached to the ceiling of the box, roughly 12 cm away from the PMT, pointing directly at it. The LED is soldered to a coaxial cable, and driven by an arbitrary waveform generator. Throughout the box, three temperature sensors and one temperature/aerial-humidity sensor are spread out. The temperature/humidity sensor is placed directly on the PMT's mounting bracket. Two more temperature sensors are placed in opposing corners on the box's ground. The last temperature sensor is fixed to the box's ceiling.

All cables are led out of the box through a light trap. The entire box is then placed within a climate chamber, which serves to cool down the setup to desired temperatures. The cables are led out of the climate chamber through a hole that is closed with a foam plug. The entire chamber is sealed and additionally covered off with a black cloth. The temperature and humidity sensors are connected through simple data cables to a DAQ box, which is connected to a PC by USB.

The PCs, power source, waveform generator and oscilloscope are all outside of the climate chamber.

Measurement

The climate chamber is used to reduce temperature in 10 °C steps, starting at room temperature of 20 °C and ending at −30 °C, covering the temperature range encountered in IceCube. After each temperature step, temperature is monitored until it is stable over 5 minutes before commencing the measurement. At each respective temperature value, data is taken with the PMT's HV set to Nominal Voltage at room temperature, and then at HV values of 50 V and 100 V higher and lower respectively. Exact temperature and humidity values are also recorded manually at the start of each measurement to account for minor, delayed variations in temperature.

Measurement is done in pulse mode, so voltage is measured. The oscilloscope is triggered on the waveform generator's signal, and focused on time-span and amplitude of the expected signal. Then, the oscilloscope records the resulting waveforms in sequence mode, which are then transferred to the laboratory PC. 50 000 such waveforms are collected for each temperature/voltage pair.

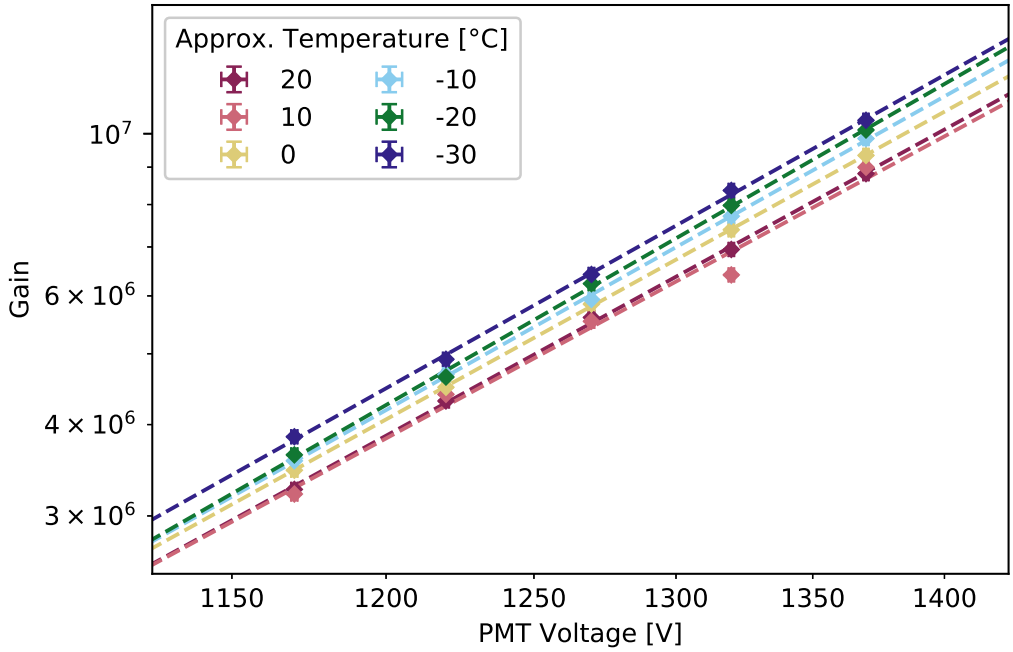

Figure 6: *Gain over Voltage and Temperature. Errorbars not plotted are smaller than the respective marker. Dotted lines are fitted exponential functions.*

Analysis and Results

For data analysis, the PeeEmTee package by Jonas Reubelt is used [10].

During calibration of the oscilloscope, a time range is determined that encompasses the entirety of the signal. Each recorded waveform is then integrated over the signal time-range to calculate the charge of the signal. A pre-signal time range is also chosen, integrated over and subtracted from the signal to filter out any baselines caused by background. The resulting charges of each waveform are then combined into a histogram. As described in subsection 2.3, the charge spectrum is made up of a number of Gaussian distributions for the background pedestal and the events caused by actual detected photons. Therefore, the charge histogram is then fitted with a number of Gaussian curves to determine further characteristics such as pedestal location and SPE location.

The first characteristic investigated is gain over temperature. As the charge of the SPE peak describes the final amount of electrons resulting from a single initial electron, it is equivalent to the gain.

Figure 6 and Figure 7 show the gain values as function of temperature and voltage. It is apparent that the gain per voltage increases with decreasing

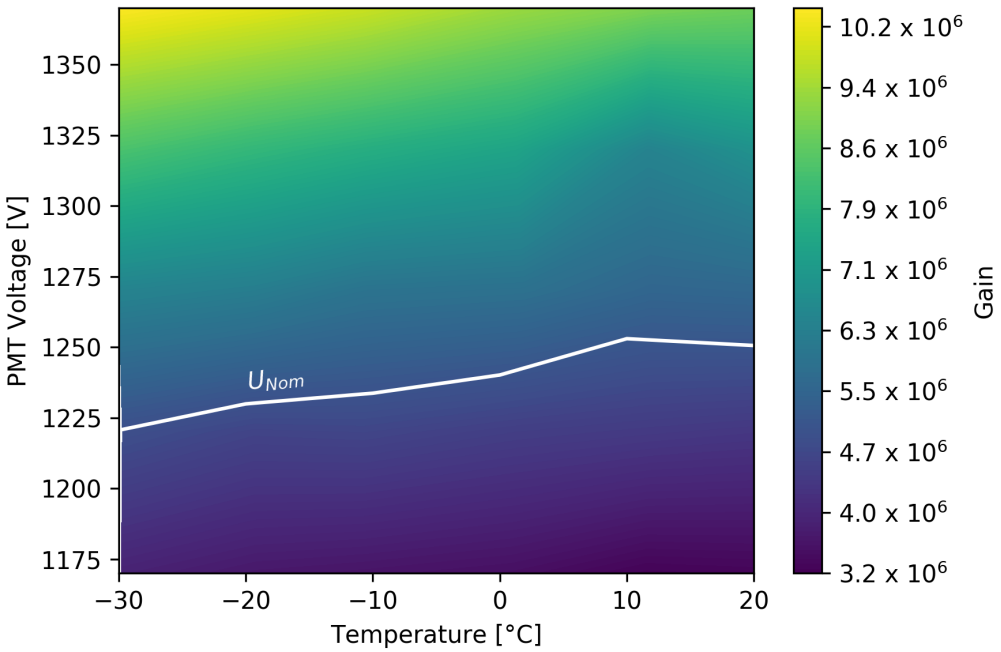

Figure 7: *Gain over Voltage and Temperature (interpolated)*

temperature. This possibly occurs due to the decreased resistance and therefore increased effectiveness of electronic components of the base at lower temperature.

Accordingly, it is of no surprise that the nominal voltage decreases with decreasing temperature, as seen in Figure 8

The second characteristic investigated is the width σ of the SPE peak. A change in peak width indicates a change in amplification behavior in the dynode system. As shown in Figure 9, sigma does not consistently change under changes in temperature. In Figure 10 any hypothetical changes of σ over temperature are smaller than the variance observed.

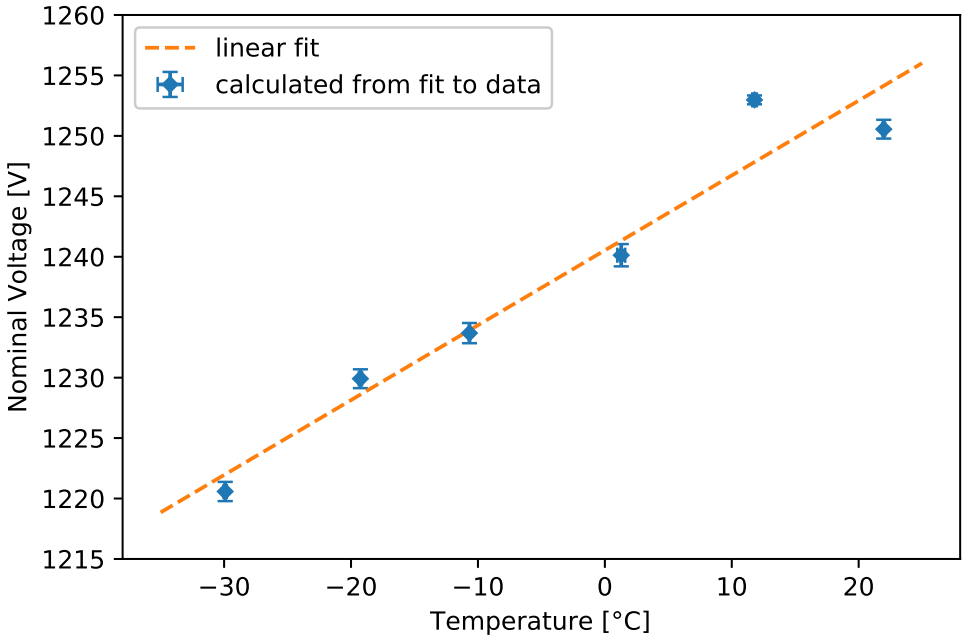

Figure 8: *Nominal Voltage over Temperature. Errorbars not plotted are smaller than the respective marker.*

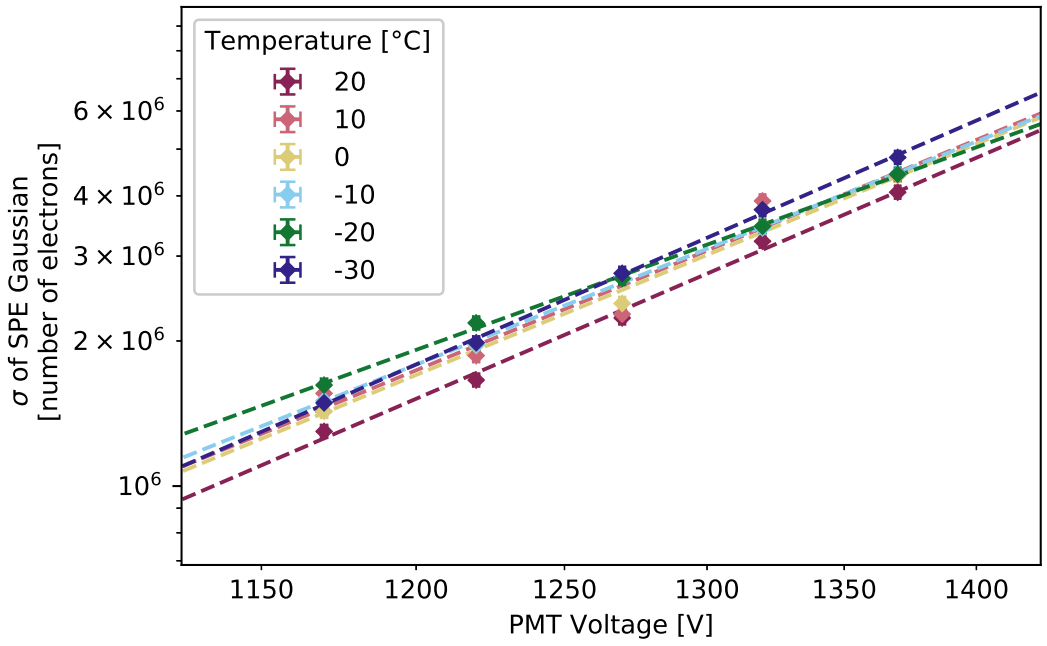

Figure 9: *σ over Voltage over Temperature. Errorbars not plotted are smaller than the respective marker. Dotted lines are fitted exponential functions.*

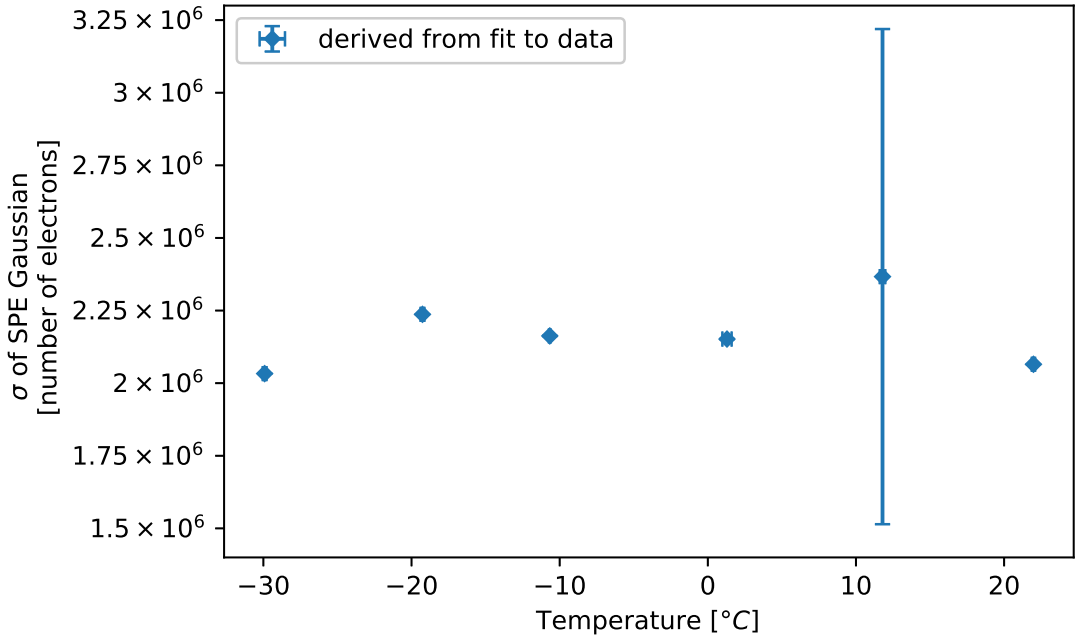

Figure 10: *σ at Nominal Voltage over Temperature, derived from the fits in the top plot. Errorbars not plotted are smaller than the respective marker. The large error at 10 °C stems from that measurement containing an outlier (see: Figure 6), which increases fitting errors.*

4 Angular acceptance

The following chapter contains experiments that investigate angular response. Understanding of angular response is essential, as reconstruction of signal geometry is vital to gaining insights into the origin of a detected neutrino.

4.1 Justification for the use of current-mode over pulse-mode

Firstly, a comparison between pulse-mode and current-mode measurement of angular response is presented to justify the use of current-mode in later measurements.

Setup

For exact equipment and settings used, see section A.

This measurement is conducted in a dark chamber, a light tight room with walls painted black. The Hamamatsu R12199-01HA PMT is mounted on an optical rail. It is connected to a HV source by coaxial cable and run at nominal voltage at room temperature. The signal is transferred by coaxial cable as well, and read by a picoampere meter for the current-mode measurement, and an oscilloscope for the pulse-mode measurement. The same cable is used for both modes, with the only difference being an adapter mounted directly before the port of the respective instrument.

The PMT's optical rail is mounted on a horizontal rotary plate, which is movable by a digitally controlled stepper motor down to sub-degree steps. The stepper is connected to a power source via a regular laboratory cable. It is controlled by two USB cables connected to the laboratory PC, one controlling the stepper itself and one linked to the stepper's encoder, which is used to measure the degrees moved. The PMT is placed at one end of the room.

A generic blue LED attached to a diffusor is positioned at a distance of roughly 3 m from the PMT. The diffusor along with the distance to the PMT ensure that the illumination is uniform. The PMT is controlled by an arbitrary waveform generator, being run in pulse-mode with 20 ns pulse width.

Measurement

The measurement in current-mode is performed with the PMT being rotated around its axis horizontally in 1° steps. After every step, the picoampere

meter records ten points of data and transmits them to the laboratory PC via the latter's DAQ card, where their mean and standard deviation are recorded.

The PMT is rotated clockwise from its initial position facing the LED frontally to an extreme angle of 135°, then counterclockwise up to an angle of −135° passing through the 0° mark, and then clockwise back to its initial position facing the LED.

Preliminary measurements indicated the presence of a background rate variable with angle in current-mode measurements, most likely due to minor leaks of light in the dark chamber. To filter this background, a dark scan is performed by performing another current-mode measurement without activating the LED. This scan allowed subtraction of the angular background in all later current-mode measurements.

Due to the considerably higher amount of time required for pulse-mode measurements, the scan in pulse-mode is conducted in 5° steps, and most angles are only scanned once. After every step, 50 000 waveforms are recorded by the oscilloscope and read out via Ethernet cable by the lab PC.

Different peak amplitudes of the LED pulses are used for current- and pulse-mode. A current-mode measurement with the low flux required for good fitting in pulse-mode sees noise with a strength reaching that of the signal, while a high flux prevents accurate fitting of pulse-mode data due to multi-photon events dominating over single-photon and pedestal events.

Analysis and results

Analysis of the pulse-mode data is analogue to the procedure described in section 3.

Notably, due to the overall higher flux and noise, directly fitting the pulse data is not accurately possible. Therefore, locations and standard deviations for the Gaussian functions corresponding to the pedestal and single photo electron events are initially determined for the data of a single extreme angle, and then fixed for the fits of all other angles. From this improved fit, the number of photoelectrons is determined, with errors being derived from the covariance results of the fit.

In current-mode, data is binned into 1° wide bins. Current errors are propagated from the initially recorded errors of the individual data points. Angular errors for both modes are omitted. As the stepper demonstrates a great accuracy, deviation in angular movement is low. Since the stepper moves in both direction, any deviations that do happen average out over time. Preliminary testing of the stepper demonstrates angular accuracy in the range of ±1° over an entire measurement (540 steps).

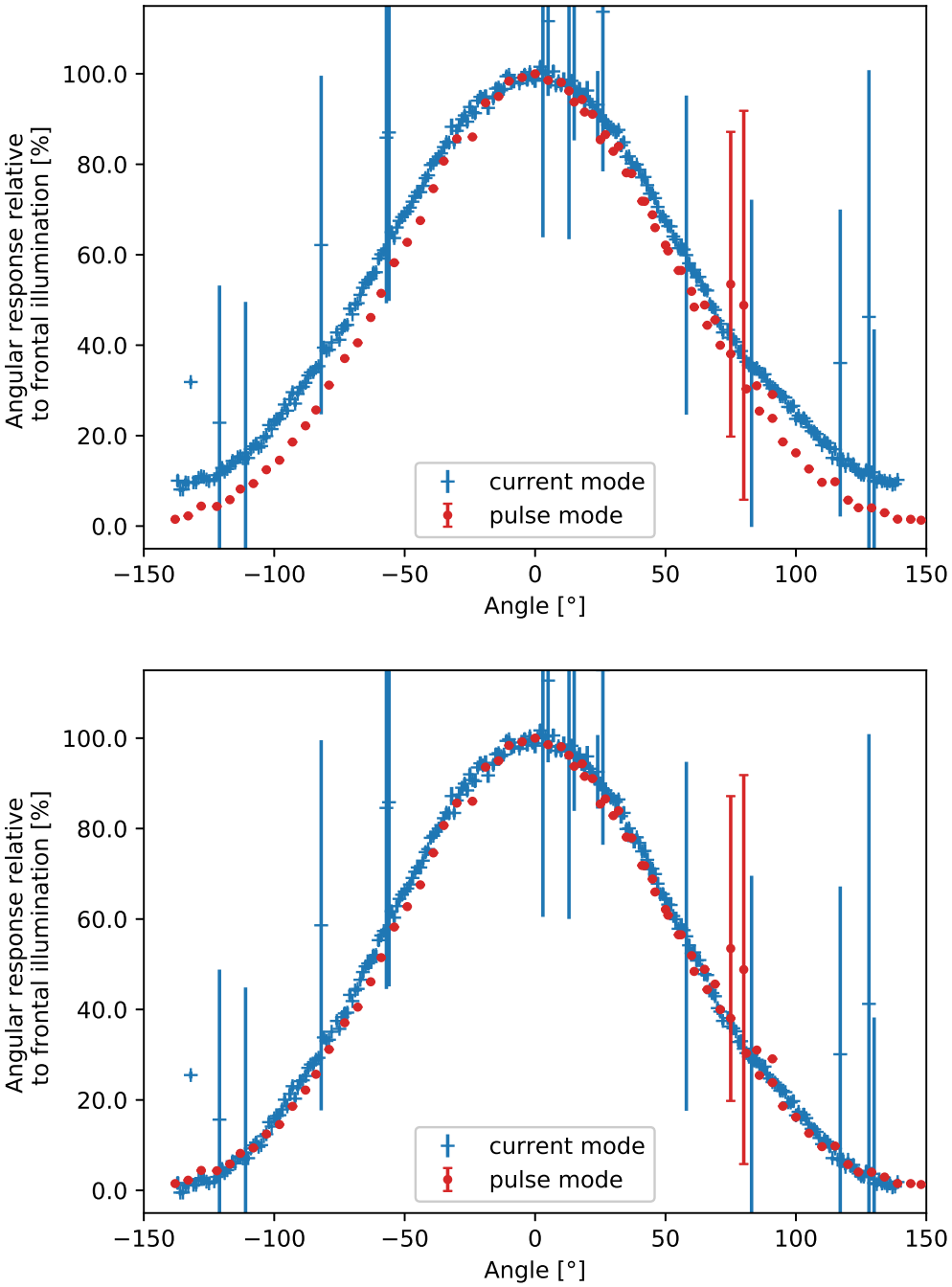

Figure 11: *Comparison of pulse-mode and current-mode. Errorbars not plotted are smaller than their marker.*
Above: *Comparison without correction of current-mode offset.*
Below: *Comparison with corrected current-mode data.*

As current- and pulse-mode measurements used different peak amplitudes for LED pulsing, no direct comparison is possible. Therefore, both sets of data were normalized, i.e. scaled to frontal exposure to the LED. Additionally, to correct any possible initial offset in angle, both sets of data are centered on their peak under the assumption that response is strongest when the PMT faces the LED under an angle of 0°.

As can be seen in Figure 11, there appears to be a difference in pulse- and current-mode data. Current-mode data shows a greater acceptance at high angles. Integration in current-mode includes a longer period of time , while in pulse-mode, the bounds for integration can be set accurately around the signal. This offset therefore can be explained by photons reflected in the dark chamber and other such non-signal noise before and after the signal. Amplitude of that noise can be found by considering the signal in current-mode at the angles at which the pulse-mode response reaches zero. This noise offset is then subtracted from all current-mode data to create comparability with pulse-mode data.

The few outlier with great errors in current-mode possible result from physical shocks to the picoampere meter, which can create one-off spikes of noise. The outliers in pulse-mode data stem from bad fits.

As precise pulse forms are not relevant for the following considerations, current-mode is used for further measurements.

4.2 Comparison of angular acceptance of HZC and Hamamatsu PMTs

To compare angular behavior of the new generation of HZC XP82B3F PMTs to the currently used Hamamatsu PMTs, angular response is measured for three HZC PMTs and a Hamamatsu PMT as comparison.

Setup

For specific equipment and settings used, see section A.

The setup remains the same as in section 4.1. The measurement is repeated with the Hamamatsu PMT being swapped with three different HZC PMTs of the type XP82B3F successively. All PMTs were operated at their respective nominal voltage. Data taking was accomplished by picoampere meter, connected to PC via DAQ card.

Measurement

The measurement was performed analogue to section 4.1.

As preliminary measurements indicate a possible drift of LED output over time, a calibration was performed, by repeating measurement with the first PMT to be measured at the end of the test series. This allows to interpolate a hypothetical LED drift and scale the measurements in between accordingly.

Results

The calibration shown in Figure 12 indicates that LED drift has no impact on this measurement.

Angular response of the four PMTs is shown in Figure 13. As the total amplitudes of the response are different, all four datasets are presented normalized to allow comparison of shape. The response of the Hamamatsu PMT lies between that of the HZC PMTs, indicating that angular response does not meaningfully differ.

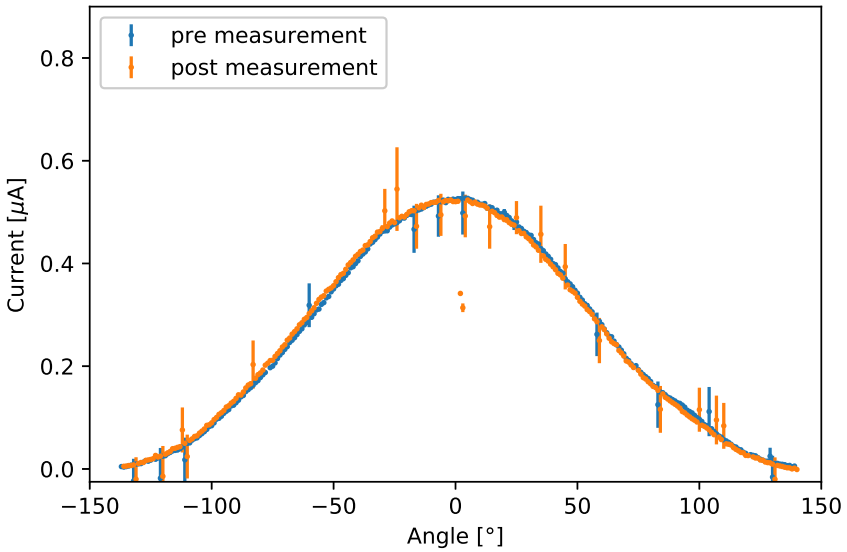

Figure 12: *Calibration measurement. Pre-measurement was taken immediately before the test series, post-measurement immediately after, with the LED remaining active throughout. Errorbars not plotted are smaller than their marker.*

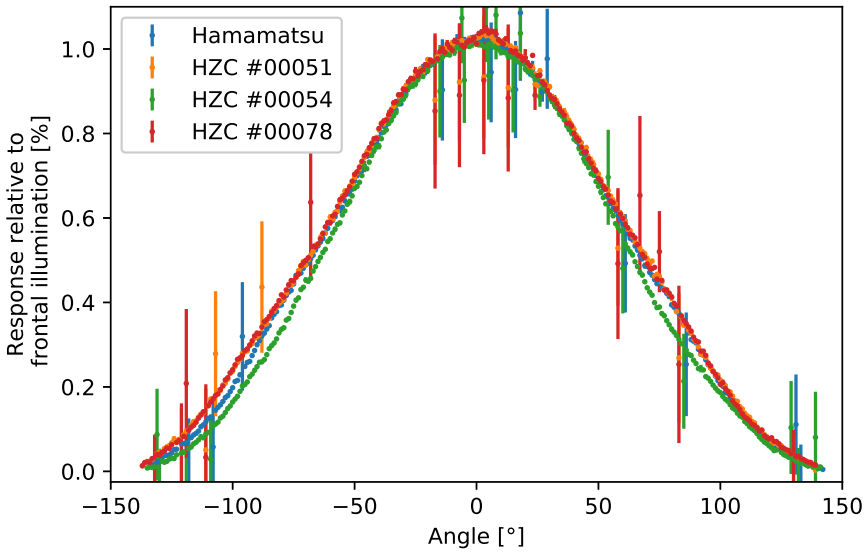

Figure 13: *Comparison of three HZC PMTs to a Hamamatsu PMT. Errorbars not plotted are smaller than their marker. All data was normalized.*

4.3 Influence of support structure reflector ring on the angular response

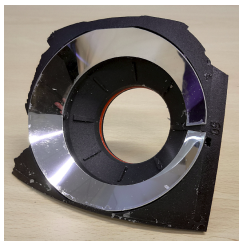

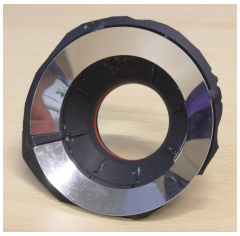

Figure 14: ***Left:*** *Ellipsoid support structure.* ***Right:*** *Circular support structure.*

In an mDOM, PMTs are mounted within a support structure to fix them in place. Two variants of the mounting structure - a circular one and an ellipsoid one - exist. The support structures are shown in Figure 14. This is necessary, as the DOMs hull is spherical around its poles and cylindrical around its equator. To increase the effective area, this support structure possesses a conical geometry and is equipped with a reflector ring to reflect additional photons onto the PMTs entrance window. These reflector rings are compared in this investigation.

Setup

The setup again is overall identical to section 4.1. The Hamamatsu PMT was used for all measurements.

Measurement

The measurement is performed as described in section 4.1. The aim of this measurement is to compare absolute current values, but preliminary measurements indicate the possibility of a drift of the LED intensity over time. To correct such a drift, measurement without supporting structure was performed at the very beginning and repeated at the end of the series of scans. By comparing these otherwise identical scans, a possible drift can be corrected.

Results

Figure 15 presents the results of the calibration measurements. It can be observed that no significant drift occurred during the test series, therefore the other data sets are presented as recorded. The outlying points of data

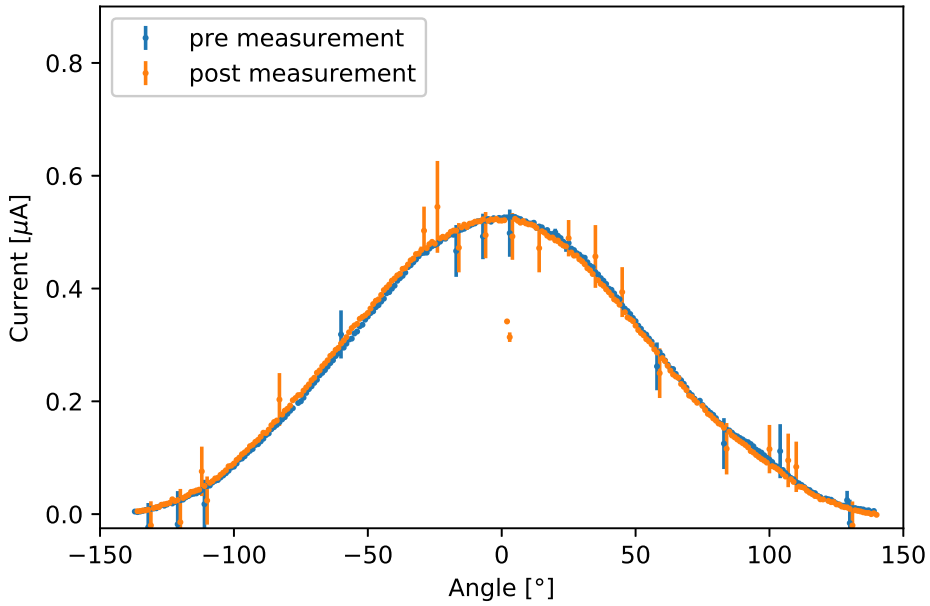

Figure 15: *Calibration measurement with the Hamamatsu PMT, to correct for possible drift of the LED. Pre-measurement was taken immediately before the test series, post-measurement immediately after, with the LED remaining active throughout. Errorbars not plotted are smaller than their marker.*

with the greater errorbar are most likely the result of physical disturbances the picoampere meter, which can cause spikes in its measurements.

The first comparison presented is that of the PMT without any mounting structure, with the circular structure, and with the ellipsoid structure. It is evident that the reflective rings in the structure greatly increase the sensitivity for angles between $-50°$ and $50°$. In this range, additional light is reflected onto the photo cathode, increasing the signal.

As the angle moves beyond those values, response is reduced compared to the signal without structure, as the outer side of the structure begins to obstruct light that would have reached the cathode at a flat angle otherwise.

Lastly, the structures create an actual hard cutoff at roughly $\pm 100°$ for the signal at the angles at which the entrance window is fully shadowed by the mounting structure. Without the structure, a low flux of light still reaches the photo cathode at very flat angles and through refraction at the entrance window.

Differences between the two variants of mounting structure are evidently

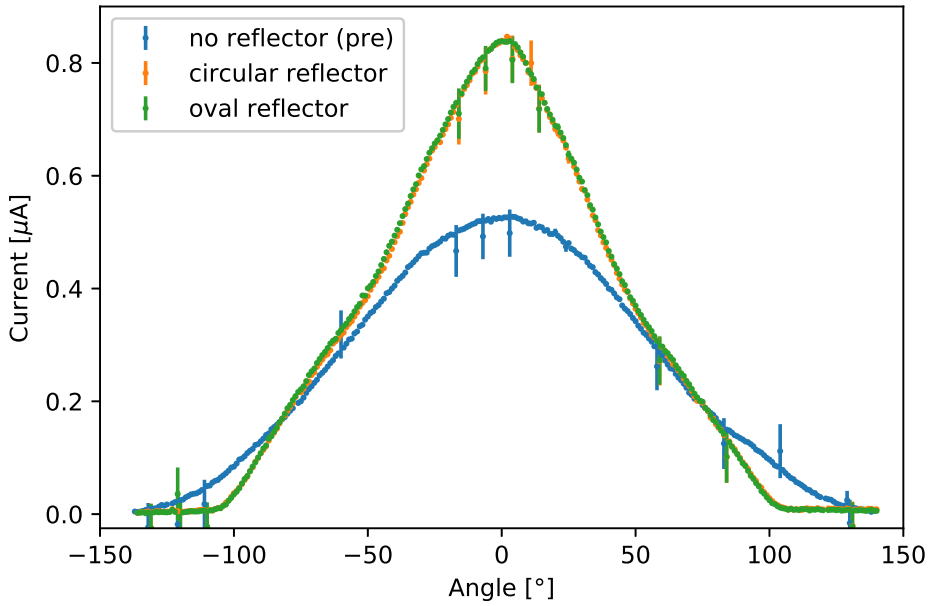

Figure 16: *Comparison of no mounting structure, circular mounting structure, and ellipsoid mounting structure. Circular and ellipsoid data are almost identical.*

minor.

As the ellipsoid mounting structure is not symmetrical under rotation, a comparison between two alignments is presented in Figure 17. The first is a vertical alignment with the broader part of the ellipsoid being oriented downwards, orthogonal to the plane of rotation. The second is a horizontal alignment with the broader part being oriented clockwise towards the angles presented as positive in this notation.

It is apparent that at low angles, the two variants mostly coincide. At angles over ±50°, the horizontal alignment provides a stronger signal at positive angles, where the "broad" part of the ellipsoid receives stronger illumination, and a weaker signal at negative angles, as the "thin" part of the ellipsoid faces the light source.

The cutoff is also slightly shifted, with the steeper edge of the thin side of the structure reaching an interposing position earlier.

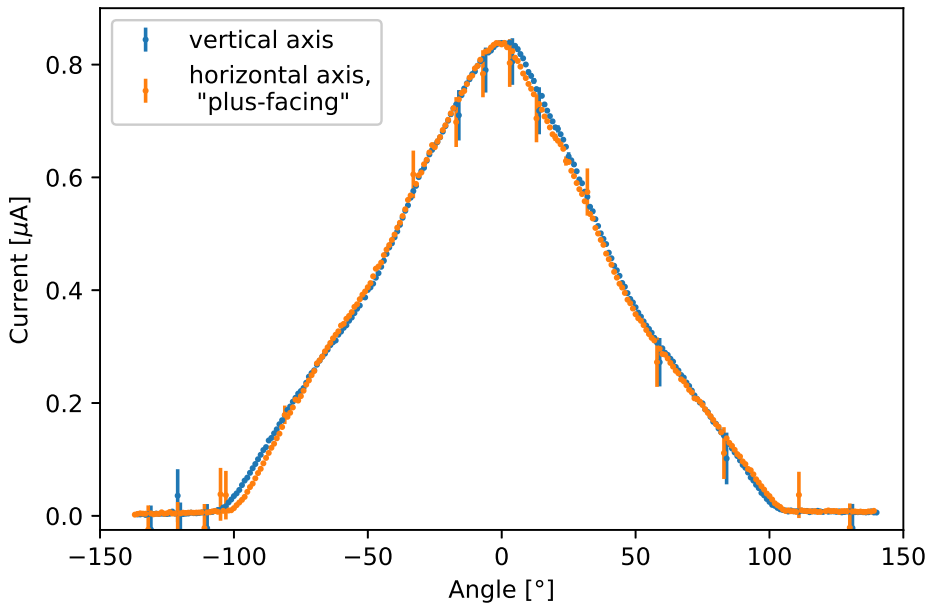

Figure 17: *Comparison of alignment of ellipsoid structure alignment. Horizontal alignment reaches a cutoff earlier at negative angles, and later at positive angles.*

5 Conclusion

Temperature dependent gain behavior was presented for a candidate PMT for the IceCube upgrade, the HZC XP82B3F. As expected, the nominal voltage was temperature dependent. The sigma of the SPE Gaussian showed no clear temperature dependence.

Equivalence of quantum efficiency in current-mode and pulse-mode measurements was verified. Current-mode measurements saw a higher baseline of noise. This baseline, however, could be subtracted to allow comparison to pulse mode response.

Angular response of the HZC XP82B3F and the Hamamatsu R12199 was compared. Measurement demonstrated that differences in angular response shape are negligible. This allows the use of existing analytical tools with the HZC XP82B3F.

Lastly, it was presented how the mounting structure affects the angular response. The addition of a reflector rings provides an increase in angular sensitivity for small angles, increasing the directional sensitivity of the mDOM. For large angles, the acceptance diminishes, due to the support structure covering a significant amount of the photocathode of the PMT. As the support structure is necessary for construction of an mDOM, the addition of the reflector ring provides no downsides. The angular sensitivity of a PMT with elliptical reflector ring is slightly asymmetrical.

References

Articles

[1] E.H. Bellamy et al. "Absolute calibration and monitoring of a spectrometric channel using a photomultiplier". In: *Nuclear Instruments and Methods in Physics Research Section A: Accelerators, Spectrometers, Detectors and Associated Equipment* 339.3 (1994), pp. 468–476. ISSN: 0168-9002. DOI: https://doi.org/10.1016/0168-9002(94)90183-X. URL: http://www.sciencedirect.com/science/article/pii/016890029490183X.

[3] IceCube-Gen2 Collaboration. "IceCube-Gen2: A Vision for the Future of Neutrino Astronomy in Antarctica". In: (2014). arXiv: 1412.5106 [astro-ph.HE].

[4] M.G. The IceCube Collaboration: Aartsen et al. "The IceCube Neutrino Observatory: instrumentation and online systems". In: *Journal of Instrumentation* 12.03 (Mar. 2017), P03012–P03012. ISSN: 1748-0221. DOI: 10.1088/1748-0221/12/03/p03012. URL: http://dx.doi.org/10.1088/1748-0221/12/03/P03012.

[5] Aya Ishihara. "The IceCube Upgrade – Design and Science Goals". In: (2019). arXiv: 1908.09441 [astro-ph.HE].

Literature

[2] Hamamatsu Photonics K.K. Editorial Committee. *PHOTOMULTIPLIER TUBES Basics and Applications*. Hamamatsu Photonics K.K. Electron Tube Division, Aug. 2007.

[8] S.O. Flyckt and C. Marmonier. *PHOTOMULTIPLIER TUBES principles & applications*. Brive, France: Photonis.

Web Sources

[6] IceCube Collaboration. *The IceCube Neutrino Observatory*. URL: http://gallery.icecube.wisc.edu/web/var/albums/Press-Root-Album/Detector/ArrayWSeasonsLabelsAmanda.jpg?m=1371067618. (accessed 9.1.2020).

[7] The IceCube Collaboration. *IceCube Quick Facts*. URL: https://icecube.wisc.edu/about/facts. (accessed 10.12.2019).

[9] U Münster. *multi-PMT DOM*. URL: https://www.sense-pro.org/images/Portraits/institutes/IC/mDOM_exploded_view-2.pdf.png. (accessed 4.1.2020).

[10] Jonas Reubelt. *PeeEmTee, Auxiliary package for PMT analyses*. URL: https://github.com/JonasReubelt/PeeEmTee. (accessed 4.1.2020).

A Equipment and detailed settings used

Specific equipment used for measurement of temperature dependent gaincurve

- PMT:
  HZC XP82B3F, Serial Number: #00051

- Base:
  Testing base built in house
  Divider ratio:

Electrodes:	K	Dy1	…	Dy8	Dy9	Dy10	P
Ratio:	3	1	1	1	1	1	
Capacitors in µF				0.01	0.01	0.01	

  K: Cathode, Dy: Dynode, P: Anode

- Oscilloscope:
  LeCroy Waverunner 6100

y-resolution	10 mV/div
TBase mode	sequence mode, 500
x-resolution	20 ns/div
trigger	external (on waveform generator's sync), 230 mV

- Arbitrary waveform generator driving the LED:
  Agilent 33220A

shape	pulse
frequency	1 kHz
highlevel for 10° and above	1.570 V
highlevel for 0° and below	1.630 V
low-level	0 V
pulse width	20 ns
edge width	5 ns

- High-voltage source supplying the PMT:
  C.A.E.N Mod. SY403

Voltage	1270 V

- Thermometer and air-humidity sensor:
  Phidget P/N 1124 and Phidget P/N 1125

- DAQ box reading out the thermometers and air-humidity sensor:
  Phidget Interface Kit 8/8/8 1018_2

Specific equipment used for justification of current-mode

pulse-mode measurement

- PMT:
  Hamamatsu R12199-01HA, Serial Number: BA0490

- Base:
  Testing base built in house
  Divider ratio:

Electrodes:	K	Dy1	…	Dy8	Dy9	Dy10	P
Ratio:	3	1	1	1	1	1	
Capacitors in µF				0.01	0.01	0.01	

  K: Cathode, Dy: Dynode, P: Anode

- Oscilloscope:
  LeCroy Waverunner 6100

y-resolution	10 mV/div
TBase mode	sequence mode, 500
x-resolution	20 ns/div
trigger	external (on waveform generator's sync), 230 mV

- Arbitrary waveform generator driving the LED:
  Agilent 33220A

shape	pulse
frequency	1 kHz
highlevel	1.8 V
low-level	0 V
pulse width	20 ns
edge width	5 ns

- High-voltage source supplying the PMT:
  C.A.E.N Mod. SY403

Voltage	1101 V

current-mode measurement

- PMT:
  Hamamatsu R12199-01HA, Serial Number: BA0490

- Base:
  Testing base built in house
  Divider ratio:

Electrodes:	K	Dy1	…	Dy8	Dy9	Dy10	P
Ratio:	3	1	1	1	1	1	
Capacitors in µF				0.01	0.01	0.01	

  K: Cathode, Dy: Dynode, P: Anode

- Picoampere-meter:
  Keithly 487

range	2 μA
integration	line cycle integration; 20 ms

- Arbitrary waveform generator driving the LED:
  Agilent 33220A

shape	pulse
frequency	1 kHz
highlevel	2.4 V
low-level	0 V
pulse width	20 ns
edge width	5 ns

- High-voltage source supplying the PMT:
  C.A.E.N Mod. SY403

Voltage	1101 V

Specific equipment used for comparison of angular response of HZC and Hamamatsu PMTs

- PMTs:
  Hamamatsu R12199-01HA, Serial Number: BA0490
  HZC XP82B3F, Serial Numbers: #00051, #00054, #00078

- Base:
  Testing base built in house
  Divider ratio:

Electrodes:	K	Dy1	…	Dy8	Dy9	Dy10	P
Ratio:	3	1	1	1	1	1	
Capacitors in µF				0.01	0.01	0.01	

K: Cathode, Dy: Dynode, P: Anode

- Picoampere-meter:
  Keithly 487

range	2 μA
integration	line cycle integration; 20 ms

- Arbitrary waveform generator driving the LED:
  Agilent 33220A

shape	pulse
frequency	1 kHz
highlevel	2 V
low-level	0 V
pulse width	20 ns
edge width	5 ns

- High-voltage source supplying the PMT:
  C.A.E.N Mod. SY403

Voltage (Hamamatsu)	1101 V
Voltage (HZC 00051)	1236 V
Voltage (HZC 00054)	1226 V
Voltage (HZC 00078)	1203 V

Specific equipment used for measurement of mounting structure reflector ring influence on angular response

- PMT:
  Hamamatsu R12199-01HA, Serial Number: BA0490

- Base:
  Testing base built in house
  Divider ratio:

Electrodes:	K	Dy1	…	Dy8	Dy9	Dy10	P
Ratio:	3	1	1	1	1	1	
Capacitors in µF				0.01	0.01	0.01	

K: Cathode, Dy: Dynode, P: Anode

- Picoampere-meter:
  Keithly 487

range	2 μA
integration	line cycle integration; 20 ms

- Arbitrary waveform generator driving the LED:
  Agilent 33220A

shape	pulse
frequency	1 kHz
highlevel	3 V
low-level	0 V
pulse width	20 ns
edge width	5 ns

- High-voltage source supplying the PMT:
  C.A.E.N Mod. SY403

Voltage (Hamamatsu)	1101 V

B Danksagung

An dieser Stelle möchte ich meine Dankbarkeit an all jene ausdrücken, die mich in der Erstellung dieser Arbeit unterstützt haben. Mein besonderer Dank gilt

Prof. Dr. Gisela Anton, für die Vergabe dieser interessanten Thematik.

Jonas Reubelt, dafür dass er mir ununterbrochen und geduldig mit seiner Expertise zur Seite stand.

Tamas Gal, dessen technische Kompetenz meinen schnellen Start in die Arbeit ermöglichte.

Meinen Kollegen aus dem Büro 341, deren Gesellschaft die Erstellung dieser Arbeit deutlich unterhaltsamer machten, und die einem immer eine gute Antwort geben konnten.

Nadja Lessing, für ihre ausdauernde Unterstützung und ihre Kommentare und Korrekturen.

C Erklärung zur ordnungsgemäßen Abfassung der vorliegenden Arbeit

Hiermit versichere ich, dass ich die vorliegende Arbeit selbständig und ohne unerlaubte Hilfe verfaßt habe.

Ich habe keine anderen als die angegebenen Quellen und Hilfsmittel benutzt und alle wörtlich oder dem Sinn nach aus anderen Texten entnommenen Stellen als solche kenntlich gemacht.

Dies gilt für gedruckte Texte ebenso wie für Texte aus dem Internet.

Die Arbeit wurde in keiner anderen Lehrveranstaltung (weder an der FAU noch an einer anderen Hochschule) in der vorliegenden oder in einer modifizierten Form vorgelegt.

Mir ist bewusst, dass jeder Verstoß gegen diese Erklärung zu einer Benotung der Arbeit mit „nicht ausreichend“ führt.

Ort, Datum

Unterschrift